

# 18F-FDG PET/CT for early prediction of pathological complete response in breast cancer neoadjuvant therapy: a retrospective analysis

Yilin Wu<sup>1,†</sup>, Yanling Li<sup>2,†</sup>, Bin Chen<sup>1</sup>, Ying Zhang<sup>1</sup>, Wanying Xing<sup>1</sup>, Baoliang Guo<sup>\*2</sup>, Wan Wang<sup>\*1</sup>

<sup>1</sup>Department of Breast Surgery, China-Japan Union Hospital of Jilin University, Changchun 130033, People's Republic of China

<sup>2</sup>Department of General Surgery, The Second Affiliated Hospital of Harbin Medical University, Harbin 150001, People's Republic of China

\*Corresponding author: Wan Wang, MD, Department of Breast Surgery, China-Japan Union Hospital of Jilin University, 126 Xiantai Street, Changchun 130033, People's Republic of China ([wwan@jlu.edu.cn](mailto:wwan@jlu.edu.cn)); or, Baoliang Guo, MD, Department of General Surgery, The Second Affiliated Hospital of Harbin Medical University, 246 Xuefu Street, Harbin 150001, People's Republic of China ([baoliangguo2013@163.com](mailto:baoliangguo2013@163.com)).

†These authors contributed equally to this work.

## Abstract

**Background:** Neoadjuvant treatment has been developed as a systematic approach for patients with early breast cancer and has resulted in improved breast-conserving rate and survival. However, identifying treatment-sensitive patients at the early phase of therapy remains a problem, hampering disease management and raising the possibility of disease progression during treatment.

**Methods:** In this retrospective analysis, we collected 2-deoxy-2-[F-18] fluoro-D-glucose (18F-FDG) positron emission tomography (PET)/computed tomography (CT) images of primary tumor sites and axillary areas and reciprocal clinical pathological data from 121 patients who underwent neoadjuvant treatment and surgery in our center. The univariate and multivariate logistic regression analyses were performed to investigate features associated with pathological complete response (pCR). An 18F-FDG PET/CT-based prediction model was trained, and the performance was evaluated by receiver operating characteristic curves (ROC).

**Results:** The maximum standard uptake values (SUVmax) of 18F-FDG PET/CT were a powerful indicator of tumor status. The SUVmax values of axillary areas were closely related to metastatic lymph node counts ( $R = 0.62$ ). Moreover, the early SUVmax reduction rates (between baseline and second cycle of neoadjuvant treatment) were statistically different between pCR and non-pCR patients. The early SUVmax reduction rates-based model showed great ability to predict pCR (AUC = 0.89), with all molecular subtypes (HR+HER2-, HR+HER2+, HR-HER2+, and HR-HER2-) considered.

**Conclusion:** Our research proved that the SUVmax reduction rate of 18F-FDG PET/CT contributed to the early prediction of pCR, providing rationales for utilizing PET/CT in NAT in the future.

**Key words:** 18F-FDG PET/CT; neoadjuvant therapy; drug response; breast cancer.

## Implications for Practice

Our study found that the 2-deoxy-2-[F-18] fluoro-D-glucose positron emission tomography /CT maximum standard uptake value reduction rate between diagnosis and the second cycle of neoadjuvant chemotherapy is a powerful pathological complete response prediction tool for breast cancer, regardless of the molecular subtypes. This finding provides insights for treatment strategies selection of patients with breast cancer and may assist clinicians in deciding the timing of surgery for neoadjuvant chemotherapy patients.

## Background

Neoadjuvant therapy (NAT) is a well-established treatment strategy for patients with early breast cancer. NAT, namely giving patients systematic anticancer therapies before surgically removing the tumor, improves the success rate of breast-conserving surgery without damaging long-term prognosis.<sup>1</sup> Recently, along with the arising of novel therapeutic targets, NAT can also serve as a platform for drug sensitivity screening.<sup>2</sup> According to the NCCN guidelines, current indications of NAT include inoperable breast cancer (inflammatory breast cancer, cN3 nodal disease, cT4 tumors, etc.) and

selected operable patients (intending to have breast-conserving surgery but with large primary tumors, cN+ disease likely to become cN0 with preoperative systemic therapy, etc.).<sup>3</sup> The surveillance of primary tumor sites using imaging examinations is of great significance during the process of NAT. Despite being the most prevalent evaluation method in clinical settings, ultrasound showed limited accuracy in predicting pathological response, possibly due to the lack of capacity to distinguish between tumor residue and chemotherapy-induced fibrosis.<sup>4</sup> Magnetic resonance imaging (MRI) is known to have a higher spatial resolution. Indeed, MRI-based

Received: 7 February 2024; Accepted: 23 May 2024.

© The Author(s) 2024. Published by Oxford University Press.

This is an Open Access article distributed under the terms of the Creative Commons Attribution-NonCommercial License (<https://creativecommons.org/licenses/by-nc/4.0/>), which permits non-commercial re-use, distribution, and reproduction in any medium, provided the original work is properly cited.

For commercial re-use, please contact [reprints@oup.com](mailto:reprints@oup.com) for reprints and translation rights for reprints. All other permissions can be obtained through our RightsLink service via the Permissions link on the article page on our site—for further information please contact [journals.permissions@oup.com](mailto:journals.permissions@oup.com).

evaluation showed a superior ability to forecast the treatment response of NAT in breast cancer.<sup>5</sup> Notably, since there is a potential risk of disease progression during NAT, adopting examine methods with promising sensitivity and specificity is critical for choosing treatment strategies that optimize patients' benefits.

Positron emission tomography (PET) directly measures the biochemical functions by quantifying the distribution of biochemical pathway-targeted probes. When performing PET, a radioactive tracer (organic molecules labeled with positron-emitting isotopes, such as oxygen-15, fluorine-18, carbon-11, etc.) was injected, and tissues with high tracer consumption were lit up in the images.<sup>6</sup> Since altered metabolism is one of the hallmarks of cancer, PET is often applied to the management of patients with cancer.<sup>7</sup> 2-Deoxy-2-[F-18] fluoro-D-glucose (18F-FDG) is a commonly used tracer, which utilizes the enhanced ability of glucose uptake in tumor cells. The FDG-consuming ability of breast cancer cells evaluated by PET/CT was proven to be associated with cancer proliferation.<sup>8</sup> 18F-FDG PET/CT has been used in diagnostic staging, metastasis detecting, and response monitoring of NAT in breast cancer. Previous studies suggested that 18F-FDG PET/CT has great sensitivity to identify larger ( $>1\text{cm}$ ) primary tumor sites but cannot replace pathological examination since the uptake ability of tumors varies with molecular and histological subtypes.<sup>9,10</sup> Moreover, 18F-FDG PET/CT might be a powerful prognosis stratification tool for patients with relatively higher-stage diseases due to its ability to differentiate distant metastases.<sup>11</sup> In NAT, a decreased rate of maximum standard uptake value (SUVmax) quantified by 18F-FDG PET/CT has been demonstrated to be related to pathological complete response (pCR) in patients with human epidermal growth factor receptor 2 (HER2)-positive breast cancer.<sup>12,13</sup> However, the usability of PET in breast cancer still waits for more clinical evidence.

In this study, early patients with breast cancer suitable for NAT were selected, and 18F-FDG PET/CT was performed before the start of NAT, after 2 cycles of NAT, and before the operation. We investigated the association between the early SUVmax reduction rate (baseline to the end of the second therapy cycle) and the total reduction rate during the NAT procedure and found that the early SUVmax reduction rate was a good representative of the total reduction rate. Besides, the early SUVmax reduction rate was closely related to pCR in our study. In conclusion, we demonstrated the prominent role of 18F-FDG PET/CT in predicting pCR in patients with breast cancer, which sheds light on the future clinical management of NAT patients.

## Methods

### Patients

One hundred and twenty-one patients with breast cancer were selected from our center between 2020 and 2023. All patients were above 18 years old, had biopsy-confirmed breast cancer, and were suitable for NAT. Standard treatment regimens were selected based on patients' clinicopathologic features. All patients have completed NAT and underwent mastectomy/breast-conserving surgery ± sentinel node biopsy (SLNB)/axillary lymph node dissection. Pathological results were reviewed by 2 pathologists independently according to the American Society of Clinical Oncology/College of American Pathologists guidelines (ASCO/CAP). PD-L1 expression

was calculated in patients with triple-negative breast cancer (TNBC) by immunohistochemistry (IHC) using the combined positive score (CPS), which quantifies the sum of PD-L1 on cancer and immune cells. Pathological complete response was defined as no invasive residual in breast and axillary lymph nodes after completion of NAT (ypT0/is ypN0). Informed consent was obtained from all patients.

### 18F-FDG PET/CT procedure

18F-FDG PET/CT was performed on each patient before NAT, after 2 cycles, and before surgical removal of the tumor site. Briefly, patients were kept fasting for 6-8 hours before injection of 18F-FDG (0.08-0.2 mCi/kg). The injection was performed through the anterior cubital vein contralateral from the primary tumor site. Patients were imaged one hour after injection. The region of interest was outlined by the intellicSpace Portal working station (Philips Medical Systems). The SUVmax value was quantified using the tumor tracking module of the workstation. All PET/CT results were reviewed by 2 experienced physicians of nuclear medicine. The SUVmax reduction rate was calculated as follows:

$$\text{SUVmax reduction rate} = \frac{(\text{PreSUVmax} - \text{PostSUVmax})}{\text{PreSUVmax}}$$

### Construction of the pCR prediction model

The total patient cohort was split into a training group and a test group at a ratio of 4:1. Significant variables in the univariate logistic regression analysis were used for model construction based on multivariate logistic regression. To avoid overfitting, the leave-one-out cross-validation method was applied to select the profile with the strongest association with clinical response. Comparisons between ROC curves were done with the pROC package.<sup>14</sup>

### Statistical analysis

Statistical analyses were done using R software (version 4.2.0). Quantitative data were tested for normal distribution and variance homogeneity using Kolmogorov-Smirnova (K-S) test. Differences between groups were analyzed using the Wilcox test or *t*-test according to the results of the K-S test. Categorical variables were assessed using the  $\chi^2$  test. *P* values less than .05 (.01 in univariate logistic regression analysis) were considered statistically significant.

## Results

### Patient characteristics and associations with pCR

In total, 121 patients with breast cancer were included between May 2020 and October 2023. The characteristics of the patients are listed in Table 1. Most patients (61%) were under 50 years old and had not experienced menopause (67%). All patients were staged IIa or above, with stage IIIc accounting for the most significant proportion (27%). Most patients (76%) had lymph node metastasis confirmed by fine-needle aspiration, and the patient cohort distributed relatively even across N stages. As for molecular subtypes, hormone receptor-positive (HR+) and HER2- were found to have the greatest number of patients (43%), whereas TNBC made up 18% of the patients. HER2+ patients comprised 39% of the cohort, with HR+HER2+ and HR-HER2+ accounting for roughly 21% and 18%, respectively. A total of 50 patients (41%) reached pCR, which was in accordance

**Table 1.** Baseline characteristics of the patient cohort.

Characteristics	Cases (%) <i>n</i> = 121	PCR status		<i>P</i> -value
		PCR	Non-PCR	
Age				
<50	74 (61%)	33	41	>.05
≥50	47 (39%)	17	30	
Menopause				
Yes	40 (33%)	13	27	>.05
No	81 (67%)	37	44	
AJCC stage				
IIa	26 (21%)	17	9	<.01
IIb	28 (23%)	15	13	
IIIa	26 (21%)	7	19	
IIIb	10 (8%)	4	6	
IIIc	31 (27%)	7	24	
T stage				
T1	13 (11%)	7	6	.04
T2	66 (55%)	33	33	
T3	23 (19%)	6	17	
T4	19 (15%)	4	15	
N stage				
N0	29 (24%)	19	10	<.01
N1	33 (27%)	18	15	
N2	24 (20%)	4	20	
N3	35 (29%)	9	26	
Subtype				
HR+HER2-	52 (43%)	8	44	<.01
HR+HER2+	25 (21%)	14	11	
HR-HER2+	22 (18%)	17	5	
TNBC	22 (18%)	11	11	
Ki-67				
<30%	19 (16%)	1	18	<.01
≥30%	102 (84%)	49	53	
PCR status				
Yes	50 (41%)			
No	71 (59%)			

with previous studies.<sup>15</sup> Features including AJCC stage, T stage, N stage, subtype, and Ki-67 index showed imbalanced distribution between pCR and non-pCR patients, indicating possible capacity to predict pCR status.

#### SUVmax reduction rate is an independent indicator of pCR

18F-FDG PET/CT evaluates the glucose metabolism of imaged tissues and has unique advantages in assessing tumor burden. To explore the potential relation between 18F-FDG PET/CT SUVmax and neoadjuvant therapy responsiveness of breast cancer, we collected SUVmax values of both primary tumor sites and axillary lymph node areas at 3 time points (baseline, after 2 cycles of neoadjuvant therapy, and after finishing standard NAT). The SUVmax reduction rates of primary breast cancer sites with/without lymph node areas between baseline and 2 cycles of NAT, baseline and preoperative, as well as 2 cycles and preoperative, were referred to as early reduction rate, total reduction rate, and late

reduction rate, respectively. Notably, the SUVmax reduction rate, including or excluding lymph node areas, showed high consistency (*R* above 0.90; Figure 1a). Overall, both early and late reduction rates showed great uniformity to the total reduction rate. The early reduction rate (*R* = 0.81) correlated better with the total reduction rate compared with the late reduction rate (*R* = 0.68; Figure 1a, 1b). The early reduction rate exhibited prominent potential in differentiating pCR and non-pCR patients. Furthermore, the early reduction rate of pCR patients was statistically higher than that of the non-pCR patients (Figure 1c, 1d). The early decrease rate also differed significantly between pCR and non-pCR groups (Figure 1d). Moreover, we found that CPS scores were higher in pCR patients and correlated positively (*R* = 0.60) with SUVmax early reduction rate and negatively (*R* = -0.35) with baseline SUVmax values in TNBC (Figure 2a, Supplementary Figure S1). Since early prediction of NAT response might change clinical decisions, we further investigated whether 18F-FDG PET/CT could provide information about pCR in the early

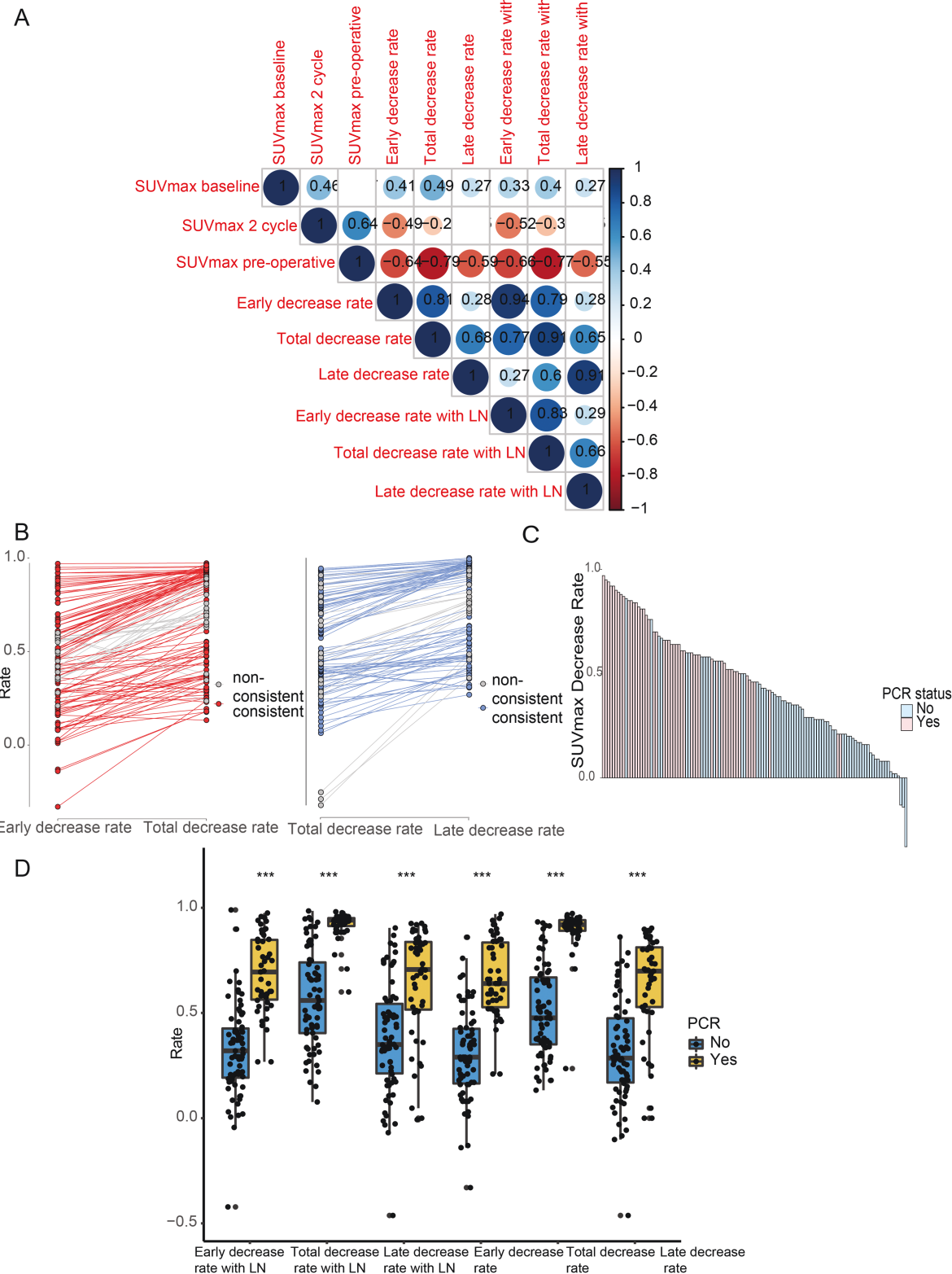


**Figure 1.** PET/CT SUVmax reduction rates differentiate pCR and non-pCR patients. (A) Correlation of SUVmax values and SUVmax reduction rates at different time points. The Spearman correlation coefficients were marked in the graph. (B) Paired correlation plots of early (left), late (right), and total reduction rates. The cases' ranks varied substantially (more than half of the number of the entire cohort) and were colored gray. (C) Early SUVmax reduction rates distribution between pCR and non-pCR patients. (D) Boxplot of SUVmax reduction rates between pCR and non-pCR groups. Abbreviations: LN, lymph node; pCR, pathological complete response; SUVmax, maximum standard uptake value. \* $P < .05$ , \*\* $P < .01$ , \*\*\* $P < .001$ .

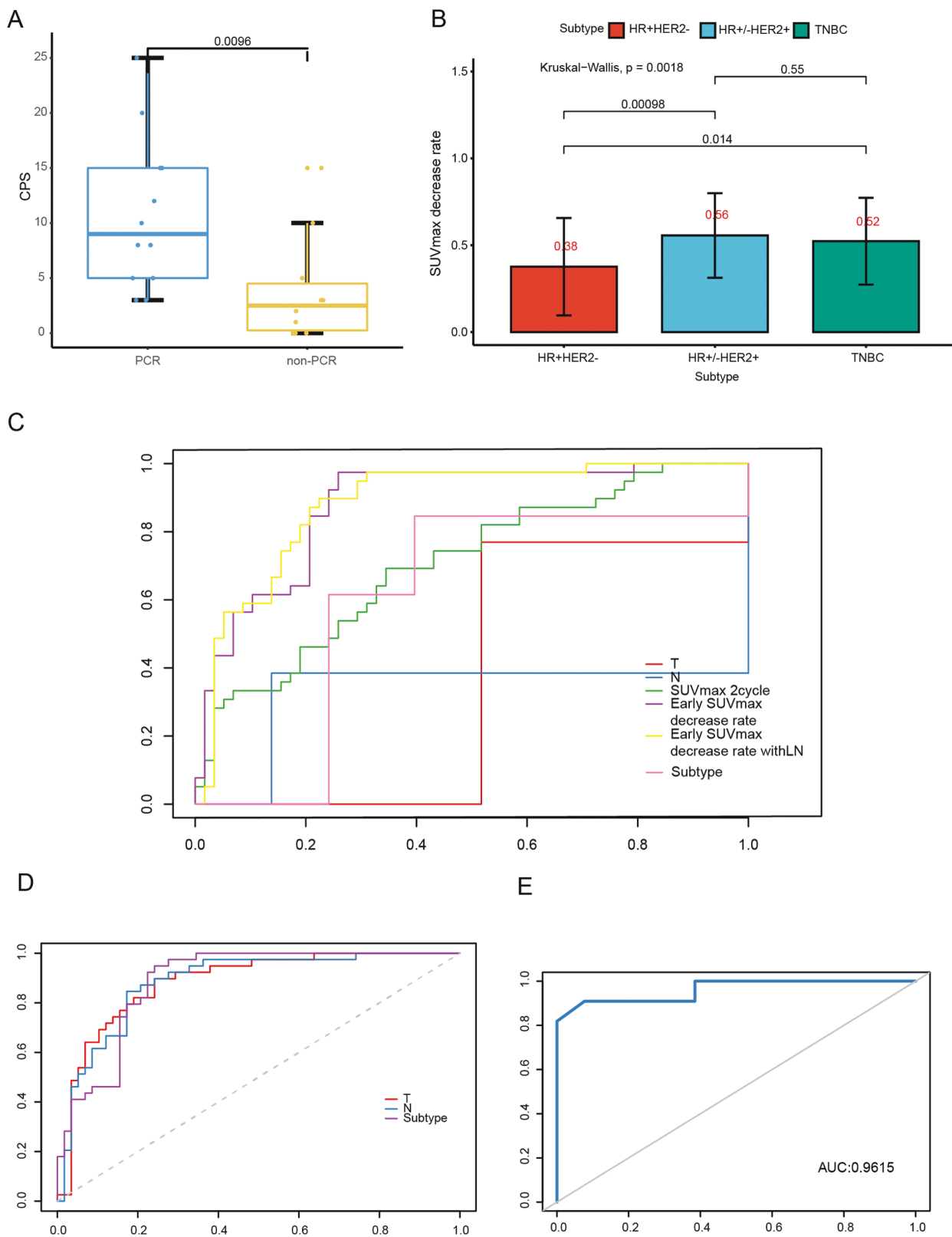


**Figure 2.** Construction of an 18F-FDG PET/CT-based pCR prediction model. (A) CPS scores of PD-L1 between pCR and non-pCR patients. (B) Early PET/CT SUV<sub>max</sub> reduction rates of molecular subtypes. (C) ROC curves of univariate logistic regression models. Sensitivity was plotted on the y-axis and 1-specificity on the x-axis. (D) ROC curves of early SUV<sub>max</sub> reduction rate-based 2 variable models. (E) ROC curve of the test group. Abbreviations: HR, hormone receptor; TNBC, triple-negative breast cancer; ROC, receiver operating characteristic; AUC, the area under the curve.

phase of treatment. In univariate logistic regression analysis, PET/CT related parameters, including SUVmax after 2 cycles of NAT and early reduction rate, along with other clinicopathological features, such as T stage, N stage and molecular subtypes and Ki-67 score, were statistically significant (Table 2). HR+HER2- patients had the lowest early SUVmax reduction rate among all subtypes (Figure 2b). Moreover, in the multivariate logistic regression analysis, the early SUVmax reduction rate was still significant, suggesting an independent predict factor of pCR (Supplementary Table S1).

### Construction of an 18F-FDG PET/CT-based neoadjuvant therapy response prediction model

To construct a PET/CT-based NAT response prediction model, variables significant in univariate logistic regression were selected for model training. We implemented the area under the ROC curve (AUC) method as the criteria for model performance. In models based on a single variable using the training set, the early SUVmax reduction rate (with both the primary tumor site and axillary lymph node site considered)

showed the highest AUC (0.88). The optimal cutoff value of the early SUVmax reduction rate was then determined by the maximum Youden index. The criterion was met when the reduction rate was at 51% (sensitivity: 0.87 and specificity: 0.80). Conversely, T stage, N stage, and molecular subtype were less effective in pCR prediction, with AUCs of 0.37, 0.33, and 0.61, respectively (Figure 2c). Multivariate model including early SUVmax reduction rate, T stage, and molecular subtype achieved the highest AUC (0.89) among all models (Figure 2d). However, the AUC did not differ statistically from the single variable model. The SUVmax reduction rate-based single variable model presented comparable performance in the test group and all molecular subtypes (Figure 2e; Supplementary Figure S2).

### 18F-FDG PET/CT identifies lymph node metastases and predicts lymph node pCR

Since axillary lymph nodes were often the first metastatic sites of breast cancer, we next explored whether 18F-FDG PET/CT can detect lymph node metastases precisely. The

**Table 2.** Univariate logistic regression to predict pCR.

Variable	PCR status		Odd ratio (OR)
	Non-PCR (N = 71)	PCR (N = 50)	
Age (Mean ± SD)	49.1 ± 10.4	45.1 ± 9.5	0.96 (0.92-1.00, P = .036)
Menopause			
Yes	27 (38%)	13 (26%)	
No	44 (62%)	37 (74%)	1.75 (0.79-3.86, P = .168)
T stage			
T1-2	39 (54.9%)	40 (80%)	
T3-4	32 (45.1%)	10 (20%)	0.30 (0.13-0.70, P = .005)
N stage			
N0	10 (14.1%)	19 (38%)	
N1-3	61 (85.9%)	31 (62%)	0.27 (0.11-0.64, P = .003)
Subtype			
HR+HER2-	44 (62%)	8 (16%)	
HR+HER2+	11 (15.5%)	14 (28%)	7.00 (2.35-20.85, P < .001)
HR-HER2+	5 (7%)	17 (34%)	18.70 (5.36-65.25, P < .001)
TNBC	11 (15.5%)	11 (22%)	5.50 (1.79-16.94, P = .003)
Ki-67 score			
<30%	18 (25.4%)	1 (2%)	
≥30%	53 (74.6%)	49 (98%)	16.64 (2.14-129.36, P = .007)
SUVmax baseline (mean ± SD)	12.6 ± 9.0	15.5 ± 7.0	1.04 (1.00-1.09, P = .070)
SUVmax 2 cycle (mean ± SD)	8.4 ± 5.9	4.8 ± 3.0	0.81 (0.72-0.91, P < .001)
SUVmax preoperative (mean ± SD)	5.6 ± 4.1	1.3 ± 0.8	0.23 (0.14-0.40, P < .001)
Early SUVmax reduction rate (mean ± SD)	0.3 ± 0.2	0.7 ± 0.2	7683.87 (327.51-180273.54, P < .001)
Total SUVmax reduction rate (mean ± SD)	0.5 ± 0.2	0.9 ± 0.1	839168.83 (4565.15-154256559.62, P < .001)
Late SUVmax reduction rate (mean ± SD)	0.3 ± 0.3	0.6 ± 0.3	68.58 (12.61-373.05, P < .001)
Early SUVmax reduction rate (with lymph node; mean ± SD)	0.3 ± 0.2	0.7 ± 0.2	6009.43 (286.62-125997.81, P < .001)
Total SUVmax reduction rate (with lymph node; mean ± SD)	0.6 ± 0.2	0.9 ± 0.1	4067067.56 (8599.55-1923477122.50, P < .001)
Late SUVmax reduction rate (with lymph node; mean ± SD)	0.4 ± 0.3	0.6 ± 0.3	50.29 (9.43-268.09, P < .001)

SUVmax values of lymph node areas varied significantly between patients with or without nodal diseases confirmed by fine-needle aspiration (Figure 3a). Moreover, the preoperative SUVmax for the lymph node area is closely related to the counts of tumor cell infiltrated lymph nodes under microscopy examination (Figure 3b). These results above indicate that 18F-FDG PET/CT could be a powerful tool to eliminate false negativity in fine-needle aspiration and SLNB.

Axillary lymph node status after NAT offers critical information on clinical decisions regarding operation procedures and postoperation treatment. To assess the predictability of PET/CT on axillary pCR (apCR), we conducted a univariate logistic analysis on multiple clinical parameters, including SUVmax values of the lymph node area only (Supplementary Table S2). The molecular subtype was found to affect apCR, with HER2+ being the most likely to accomplish apCR. Surprisingly, the early SUVmax reduction rate (with both the primary tumor site and axillary lymph node site considered), which was the most superior in predicting total pCR, still remained to obtain the highest AUC (0.93), even compared to variables focusing on the axillary area only (Figure 3c, 3d). The optimal cutoff was at 47%, with a sensitivity of 0.84 and specificity of 0.90. The model performed consistently across the test group and all molecular subtypes (Figure 3e; Supplementary Figure S1).

## Discussion

In the study we presented, our goal centered on elucidating the role of 18F-FDG PET/CT in breast cancer neoadjuvant therapy. The reduction rate of SUVmax between the start of neoadjuvant therapy and the end of the second treatment cycle was demonstrated to be a prospective predictor of pCR. This finding allows clinicians to alter treatment regimens earlier in the NAT procedure. For nonresponders predicated by the early SUVmax reduction rate, surgery might be moved up to prevent disease progression. Moreover, the high sensitivity and specificity of early SUVmax reduction rate for pCR prediction potentially provide the rationale to conduct clinical trials aiming to explore escalation therapies for treatment-insensitive patients, for instance, the combination of standard chemotherapy and targeted therapies (PARPi, anti-PD-L1, etc.). Screening sensitive patients using the SUVmax reduction rate can also contribute to therapy de-escalation. In the PHERGain trial, responders to HP treatment evaluated by 18F-FDG PET/CT can be spared from cytotoxic drugs in NAT without damaging iDFS. Such findings could decrease the occurrence of severe adverse effects in NAT patients.<sup>16</sup> Our study extended the conclusion that SUVmax reduction rate is a promising predictor for pCR to all molecular subtype patients with standard NAT regimens. This finding may facilitate the development of clinical trials investigating de-escalation therapies in other BC molecular subgroups. Admittedly, our cohort's number of patients was relatively small, and the histological subtypes were almost entirely invasive ductal carcinoma (IDC). Previous research has proved that FDG avidity was lower for invasive lobular carcinomas than IDC.<sup>17</sup> Therefore, studies with larger patient cohorts and more diversified patient characteristics were still of great importance in this field.

It is widely recognized that patients who attained pCR have improved survival.<sup>18</sup> In order to achieve pCR, selecting

suitable patients and treatment strategies are essential. Higher T and N stages and more aggressive subtypes (HER2+ and TNBC) were found to benefit more from NAT.<sup>15</sup> Besides clinical traits, great efforts have also been made to discover sensitive molecular biomarkers. Gene or protein expressions of participants in DNA methylation, mutation, and immune-related pathways have been associated with pCR status, such as MKI67 and PD-L1, which were also tested in our research.<sup>19</sup> Programmed cell death protein 1 (PD-1) interacts with its ligand (PD-L1) and promotes immune escape of tumor cells from T-cell surveillance, which has been used as therapeutics targeting malignancies.<sup>20</sup> PD-L1 expression acts as a response predictor in anti-PD-L1 immunotherapies. However, its role in chemotherapy remains relatively unknown. In lung cancer, researchers found that cytotoxic chemotherapy upregulated tumor PD-L1 expression levels, which indicated a worse prognosis.<sup>21,22</sup> Nonetheless, more patients with high levels of PD-L1 at baseline reached pCR compared with their counterparts in TNBC, whereas PD-L1 was not statistically correlated with pCR in other subtypes.<sup>23,24</sup> Since chemotherapy is considered immune-modulatory, biomarkers from immune-related biological processes might be helpful predictors for chemotherapy.<sup>25</sup>

Multiple imaging examinations have been used to evaluate tumor volumes during the NAT process. However, the efficacy of traditional methods such as physical examination and ultrasound is limited.<sup>26</sup> More advanced imaging methods, including MRI, appeared more effective.<sup>27</sup> MRI possesses high spatial resolution and can localize small breast lesions that are possibly ignored by ultrasound and mammograph. A novel imaging method, PET/MRI, might make up for the shortcomings in spatial sensitivity of PET/CT.<sup>28</sup> Large-scale clinical trials dedicated to comparing the ability of MRI, PET/CT, and PET/MRI are needed to standardize the usage of these imaging examinations.

Assessment of circulating tumor DNA (ctDNA) was considered a noninvasive way for NAT outcome prediction. ctDNA denotes fragmented DNA originating from tumor cells in the circulation system. Common releasing mechanisms of ctDNA include cell death (mainly apoptosis and necrosis)-related passive release and extracellular vesicle-associated active release.<sup>29</sup> Previous studies have proved that the level of ctDNA was positively correlated with tumor size and disease aggressiveness and predicted patients' survival in multiple cancer types.<sup>30,31</sup> Moreover, since dormant tumor cells can still be sources of ctDNA, assessing ctDNA is potentially an effective way to monitor relapse.<sup>32</sup> As for the NAT setting, Magbanua et al found that the early clearance of ctDNA 3 weeks after treatment initiation predicts a favorable response in TNBC. However, there are various challenges to conquer before the wide clinical application of ctDNA measurement for treatment responsiveness evaluation. Firstly, false negativity could be induced due to the low level of ctDNA in the bloodstream, whereas false positivity might arise from tumor heterogeneity and the influence of somatic alterations from normal cells.<sup>29</sup> Secondly, because of the unclear process of ctDNA clearance by macrophages and the debating half-life of ctDNA, the timing of ctDNA detection and cutoff values for statistically significant ctDNA reduction rate during cancer treatment remain elusive.<sup>33</sup> Thirdly, standard methods to quantify ctDNA precisely are still lacking.<sup>31</sup> Whether ctDNA can complement 18F-FDG PET/CT for early prediction of NAC response in BC, especially in histology subtypes with

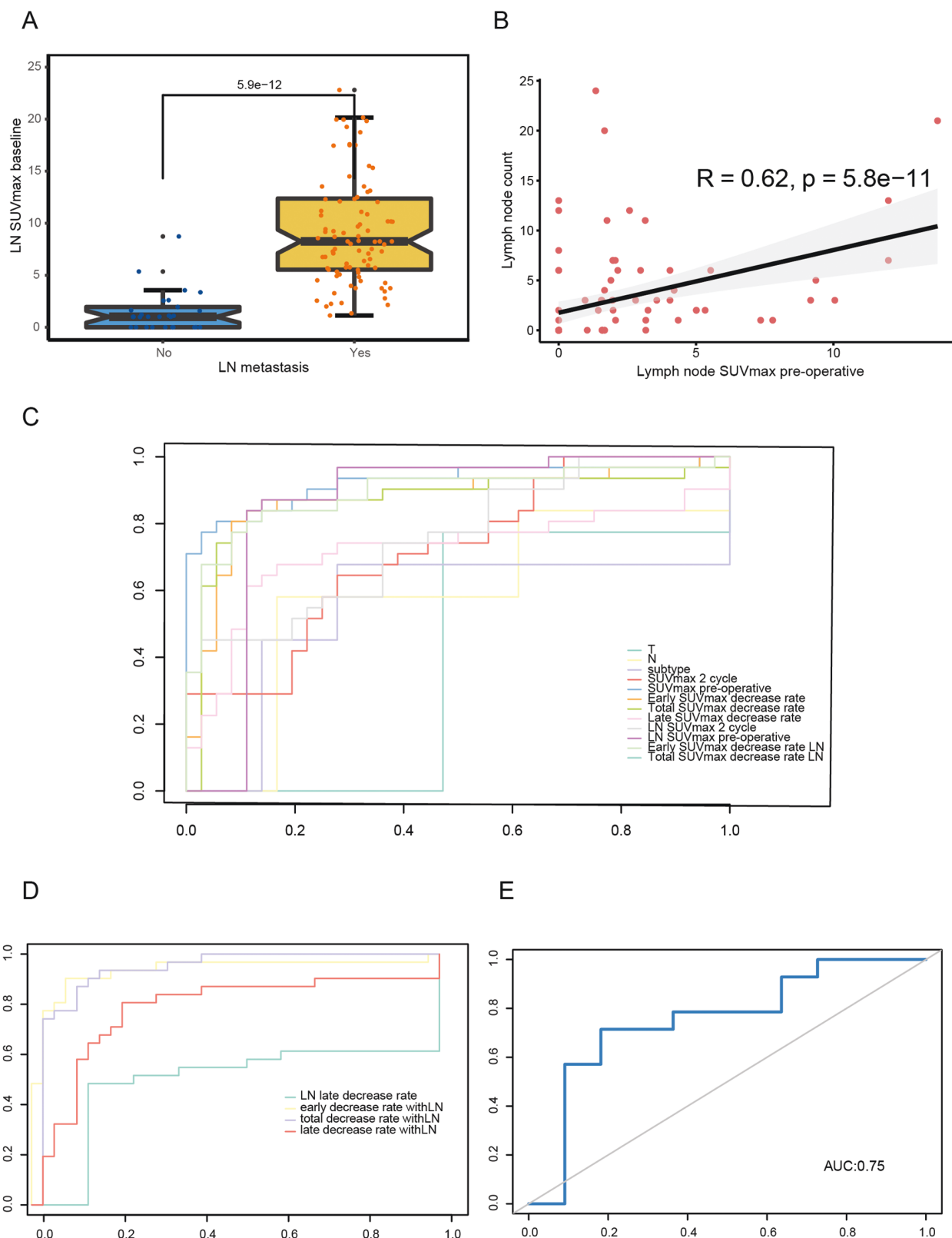


**Figure 3.** Construction of an 18F-FDG PET/CT-based axillary pCR prediction model. (A) Baseline SUVmax values of the axillary lymph node areas between patients with (right) or without (left) nodal diseases. (B) Correlation of preoperative PET/CT lymph node area SUVmax and metastatic lymph node counts using Spearman correlation. (C, D) ROC curves of univariate logistic regression models. Sensitivity was plotted on the y-axis and 1-specificity on the x-axis. (E) ROC curve of the test group.

low FDG avidity, such as lobular carcinoma, must be studied in large-scale RCTs.<sup>10</sup>

## Conclusions

In conclusion, our research proved that SUVmax values were essential indicators of tumor status. SUVmax values reflect patients' lymph node metastasis states and the SUVmax reduction rate of 18F-FDG PET/CT contributed to the early prediction of total pCR and axillary pCR. Our research provides rationales for utilizing PET/CT in NAT in the future.

## Author Contributions

Yilin Wu (Investigation, Data analysis and interpretation), Yanling Li (Investigation, Data analysis and interpretation), Bin Chen (Collection and assembly of data, Data curation), Ying Zhang (Writing—original draft, Writing—review & editing), Wanying Xing (Writing—original draft, Writing—review & editing), Baoliang Guo (Study design and administration, Writing—original draft, Writing—review & editing), and Wan Wang (Study design and administration, Writing—original draft, Writing—review & editing)

## Funding

This work was supported by Jilin Scientific and Technological Development Program [grant no. 20210101323JC].

## Conflict of interest

The authors declare no competing interests.

## Ethics approval and consent to participate

Informed consent was obtained from all patients participated in the study.

## Consent for publication

All patients consented to the publication of the manuscript.

## Data Availability

Please contact the corresponding authors for all data requests.

## Supplementary Material

Supplementary material is available at *The Oncologist* online.

## References

- Early Breast Cancer Trialists' Collaborative Group (EBCTCG). Long-term outcomes for neoadjuvant versus adjuvant chemotherapy in early breast cancer: meta-analysis of individual patient data from ten randomised trials. *Lancet Oncol.* 2018;19(1):27-39.
- Barker AD, Sigman CC, Kelloff GJ, et al. I-SPY 2: an adaptive breast cancer trial design in the setting of neoadjuvant chemotherapy. *Clin Pharmacol Ther.* 2009;86(1):97-100. <https://doi.org/10.1038/clpt.2009.68>
- Gradishar WJ, Moran MS, Abraham J, et al. Breast cancer, version 3.2022, NCCN clinical practice guidelines in oncology. *J Natl Compr Canc Netw.* 2022;20(6):691-722. <https://doi.org/10.6004/jnccn.2022.0030>
- Baumgartner A, Tausch C, Hosch S, et al. Ultrasound-based prediction of pathologic response to neoadjuvant chemotherapy in breast cancer patients. *Breast.* 2018;39:19-23. <https://doi.org/10.1016/j.breast.2018.02.028>
- Shi Z, Huang X, Cheng Z, et al. MRI-based quantification of intratumoral heterogeneity for predicting treatment response to neoadjuvant chemotherapy in breast cancer. *Radiology.* 2023;308(1):e222830. <https://doi.org/10.1148/radiol.222830>
- Mankoff DA, Katz SI. PET imaging for assessing tumor response to therapy. *J Surg Oncol.* 2018;118(2):362-373. <https://doi.org/10.1002/jso.25114>
- Hanahan D. Hallmarks of cancer: new dimensions. *Cancer Discov.* 2022;12(1):31-46. <https://doi.org/10.1158/2159-8290.CD-21-1059>
- Tchou J, Sonnad SS, Bergey MR, et al. Degree of tumor FDG uptake correlates with proliferation index in triple negative breast cancer. *Mol Imaging Biol.* 2010;12(6):657-662. <https://doi.org/10.1007/s11307-009-0294-0>
- Eo JS, Chun IK, Paeng JC, et al. Imaging sensitivity of dedicated positron emission mammography in relation to tumor size. *Breast.* 2012;21(1):66-71. <https://doi.org/10.1016/j.breast.2011.08.002>
- Hadebe B, Harry L, Ebrahim T, Pillay V, Vorster M. The Role of PET/CT in breast cancer. *Diagnostics.* 2023;13(4):597. <https://doi.org/10.3390/diagnostics13040597>
- Groheux D, Hindie E, Delord M, et al. Prognostic impact of (18)FDG-PET-CT findings in clinical stage III and IIB breast cancer. *J Natl Cancer Inst.* 2012;104(24):1879-1887.
- Hatschek T, Foukakis T, Bjöhlé J, et al. Neoadjuvant trastuzumab, pertuzumab, and docetaxel vs trastuzumab emtansine in patients with ERBB2-positive breast cancer: a phase 2 randomized clinical trial. *JAMA Oncol.* 2021;7(9):1360-1367. <https://doi.org/10.1001/jamaonc.2021.1932>
- Pérez-García JM, Gebhart G, Ruiz Borrego M, et al.; PHERGain steering committee and trial investigators. Chemotherapy de-escalation using an 18F-FDG-PET-based pathological response-adapted strategy in patients with HER2-positive early breast cancer (PHERGain): a multicentre, randomised, open-label, non-comparative, phase 2 trial. *Lancet Oncol.* 2021;22(6):858-871. [https://doi.org/10.1016/S1470-2045\(21\)00122-4](https://doi.org/10.1016/S1470-2045(21)00122-4)
- Robin X, Turck N, Hainard A, et al. PROC: an open-source package for R and S+ to analyze and compare ROC curves. *BMC Bioinf.* 2011;12:77. <https://doi.org/10.1186/1471-2105-12-77>
- Rapoport BL, Barnard-Tidy J, Van Eeden RI, et al. Pathological complete response in early breast cancer patients undergoing neoadjuvant chemotherapy: focus on Ki-67 and molecular subtypes. *Ann Oncol.* 2019;30:iii37. <https://doi.org/10.1093/annonc/mdz097.012>
- Pérez-García JM, Cortés J, Ruiz-Borrego M, et al. 3-year invasive disease-free survival with chemotherapy de-escalation using an 18F-FDG-PET-based, pathological complete response-adapted strategy in HER2-positive early breast cancer (PHERGain): a randomised, open-label, phase 2 trial. *Lancet.* 2024;403(10437):1649-1659. [https://doi.org/10.1016/s0140-6736\(24\)00054-0](https://doi.org/10.1016/s0140-6736(24)00054-0)
- Groheux D, Hindie E. Breast cancer: initial workup and staging with FDG PET/CT. *Clin Transl Imaging.* 2021;9(3):221-231. <https://doi.org/10.1007/s40336-021-00426-z>
- Cortazar P, Zhang L, Untch M, et al. Pathological complete response and long-term clinical benefit in breast cancer: the CTNeoBC pooled analysis. *Lancet.* 2014;384(9938):164-172. [https://doi.org/10.1016/S0140-6736\(13\)62422-8](https://doi.org/10.1016/S0140-6736(13)62422-8)
- Freitas AJA, Causin RL, Varuzza MB, et al. Molecular biomarkers predict pathological complete response of neoadjuvant chemotherapy in breast cancer patients: review. *Cancers (Basel).* 2021;13(21):5477. <https://doi.org/10.3390/cancers13215477>
- Vranic S, Cyprian FS, Gatalica Z, Palazzo J. PD-L1 status in breast cancer: current view and perspectives. *Semin Cancer Biol.* 2021;72:146-154. <https://doi.org/10.1016/j.semcaner.2019.12.003>

21. Guo L, Song P, Xue X, et al. Variation of programmed death ligand 1 expression after platinum-based neoadjuvant chemotherapy in lung cancer. *J Immunother.* 2019;42(6):215-220. <https://doi.org/10.1097/CJI.0000000000000275>
22. Sakai H, Takeda M, Sakai K, et al. Impact of cytotoxic chemotherapy on PD-L1 expression in patients with non-small cell lung cancer negative for EGFR mutation and ALK fusion. *Lung Cancer.* 2019;127:59-65. <https://doi.org/10.1016/j.lungcan.2018.11.025>
23. Cerbelli B, Pernazza A, Botticelli A, et al. PD-L1 expression in TNBC: a predictive biomarker of response to neoadjuvant chemotherapy? *Biomed Res Int.* 2017;2017:1750925. <https://doi.org/10.1155/2017/1750925>
24. Hussein MA, Ismail HAR, Sakr M, Nouh MA. Expression of PD-L1 in locally advanced breast cancer and its impact on neoadjuvant chemotherapy response. *Asian Pac J Cancer Prev.* 2022;23(6):2095-2103. <https://doi.org/10.31557/APJCP.2022.23.6.2095>
25. Zitvogel L, Apetoh L, Ghiringhelli F, Kroemer G. Immunological aspects of cancer chemotherapy. *Nat Rev Immunol.* 2008;8(1):59-73. <https://doi.org/10.1038/nri2216>
26. Vinnicombe SJ, MacVicar AD, Guy RL, et al. Primary breast cancer: mammographic changes after neoadjuvant chemotherapy, with pathologic correlation. *Radiology.* 1996;198(2):333-340. <https://doi.org/10.1148/radiology.198.2.8596827>
27. Gezer NS, Orbay O, Balcı P, et al. Evaluation of neoadjuvant chemotherapy response with dynamic contrast enhanced breast magnetic resonance imaging in locally advanced invasive breast cancer. *J Breast Health.* 2014;10(2):111-118. <https://doi.org/10.5152/tjbh.2014.2035>
28. Fowler AM, Strigel RM. Clinical advances in PET-MRI for breast cancer. *Lancet Oncol.* 2022;23(1):e32-e43. [https://doi.org/10.1016/S1470-2045\(21\)00577-5](https://doi.org/10.1016/S1470-2045(21)00577-5)
29. Stejskal P, Goodarzi H, Srovnal J, et al. Circulating tumor nucleic acids: biology, release mechanisms, and clinical relevance. *Mol Cancer.* 2023;22(1):15.
30. Magbanua MJM, Brown Swigart L, Ahmed Z, et al. Clinical significance and biology of circulating tumor DNA in high-risk early-stage HER2-negative breast cancer receiving neoadjuvant chemotherapy. *Cancer Cell.* 2023;41(6):1091-1102.
31. Osumi H, Shinozaki E, Yamaguchi K, Zembutsu H. Clinical utility of circulating tumor DNA for colorectal cancer. *Cancer Sci.* 2019;110(4):1148-1155. <https://doi.org/10.1111/cas.13972>
32. Ou HL, Hoffmann R, González-López C, et al. Cellular senescence in cancer: from mechanisms to detection. *Mol Oncol.* 2021;15(10):2634-2671. <https://doi.org/10.1002/1878-0261.12807>
33. Sanz-Garcia E, Zhao E, Bratman SV, Siu LL. Monitoring and adapting cancer treatment using circulating tumor DNA kinetics: current research, opportunities, and challenges. *Sci Adv.* 2022;8(4):eabi8618. <https://doi.org/10.1126/sciadv.abi8618>